Available online at www.sciencedirect.com
ScienceDirect
Ceramics International 37 (2011) 215–221
CERAMICS INTERNATIONAL
www.elsevier.com/locate/ceramint

# Calcium aluminate cement source evaluation for $Al_2O_3$–MgO refractory castables

M.A.L. Braulio, G.G. Morbioli, D.H. Milanez, V.C. Pandolfelli *

*Federal University of São Carlos, Materials Engineering Department, Materials Microstructural Engineering Group, FIRE Associate Laboratory, km 235, Rod. Washington Luís, 13565-905 São Carlos, SP, Brazil*

Received 28 May 2010; received in revised form 14 July 2010; accepted 23 August 2010
Available online 29 September 2010

**Abstract**

Alumina–magnesia refractory castables are commonly bonded with calcium aluminate cements. At temperatures above 1200 °C, these materials present an expansive behavior due to the *in situ* spinel ($MgAl_2O_4$) formation and the $CA_2$ and $CA_6$ ones. One alternative to control the volumetric stability is by replacing the typical cements used (30 wt.% CaO) for another containing less lime (20 wt.% CaO). Nevertheless, when changing the cement sources, the castable's properties would be affected. Among them, the most relevant are the green mechanical strength, the drying behavior, the properties at intermediate and high temperatures, the expansion behavior, the hot modulus of rupture and creep. Considering these aspects, the objective of this work was to evaluate the impact of different cement sources in the processing steps and properties of alumina–magnesia castables. The results pointed out specific behaviors for each cement source during the whole processing stages, highlighting the importance of its proper selection in order to attain the required properties in working conditions.


*Keywords:* C. Mechanical properties; C. Thermal expansion; E. Refractories; Calcium aluminate cements

## 1. Introduction

*In situ* spinel-forming refractory castables usually rely on a calcium aluminate cement (CAC) bonding system. The main reasons for selecting this binder are related to its placing advantages (suitable working, setting and demoulding time, as well as mechanical strength at the green stage, price and availability) [1–3].

Despite these benefits, the addition of cement must be designed in terms of content and source, as refractoriness drawbacks can arise [4]. Moreover, as calcium aluminate cement plays a role in the MgO hydration mechanism [1,5], this effect could result in further shortcomings (such as cracking and mechanical strength decrease) during curing and drying-out of magnesia-containing castables. Taking into account that this sort of castable is commonly applied in steel ladles, the cement dehydration and its effect on the mechanical strength (up to 1000 °C) must also be tracked.

At high temperatures (mainly above 1100 °C), noteworthy reactions of calcium aluminate phases take place [1]. Therefore, besides the *in situ* spinel ($MgAl_2O_4$) formation, which is usually followed by expansion [6–9], alumina–magnesia refractory castables are also prone to volumetric changes due to the $CA_2$ and $CA_6$ formation (C: CaO, A: $Al_2O_3$) [10–13]. Considering this aspect, the content, source and mineralogical composition of the calcium aluminate cement would affect the *in situ* spinel forming castables' behavior, not only during initial processing steps (curing and drying) but also at sintering temperatures.

Therefore, as calcium aluminate cement plays active roles during the overall castable's processing steps, it must be properly selected in order to ensure a suitable performance when applying the material. Different sources of cements are commercially available and they vary mainly in terms of mineralogy ($CA/CA_2$ ratio, content of $C_{12}A_7$, $Al_2O_3$ and CaO amount), particle size distribution and chemical additives [3,14,15].

In this context, this work addresses the evaluation of different calcium aluminate cement sources at different processing stages of $Al_2O_3$–MgO refractory castables. During curing, the green mechanical strength was analyzed, pointing

* Corresponding author.
*E-mail address:* vicpando@power.ufscar.br (V.C. Pandolfelli).

0272-8842/$36.00 
doi:10.1016/j.ceramint.2010.09.027

out indicatives of the CA and $CA_2$ contents in the cements. Thermogravimetrical analyses were carried out in order to evaluate the drying rate, the cement dehydration, the brucite [$Mg(OH)_2$] decomposition and the interaction between magnesia and different sources of cement.

Additionally, the behavior at intermediate temperatures (from 110 °C up to 1000 °C) was assessed in terms of mechanical strength and apparent porosity. At high temperatures (above 1000 °C), different tests were performed: cold and hot 3-point bending tests, creep resistance and the assisted sintering technique in order to evaluate the spinel and $CA_6$ formation and expansion. In all of these processing steps (curing, drying and sintering), the different sources of cements resulted in distinct properties, pointing out this variable as an option to attain the most suitable behavior for a specific application or alternative when required.

## 2. Materials and techniques

Vibratable castable compositions were formulated considering the Alfred particle packing model ($q = 0.26$) [16]. The castables' matrix comprised 6 wt.% of dead-burnt magnesia (<45 μm, 95 wt.% of MgO, $CaO/SiO_2$ ratio = 0.37, Magnesita Refratários S.A., Brazil), 1 wt.% of microsilica (971U, Elkem, Norway) and 7 wt.% of reactive alumina (CL370, Almatis, USA). Coarse tabular alumina was also used as aggregates ($d \leq 6$ mm, Almatis, USA) to complement the compositions. An electrosteric dispersing agent was added in order to ensure suitable dispersion (Basf, Germany).

Five sources of calcium aluminate cement were evaluated (6 wt.% in the castable's matrix): four of them comprising 70 wt.% of alumina and 30 wt.% of calcia (A: Secar71, Kerneos, France; B: CA270, C: CA470TI and D: CA14M, Almatis, Germany), and a fifth one containing 80 wt.% of alumina and 20 wt.% of calcia (E: Secar80, Kerneos, France). Table 1 shows the chemical analysis, physical properties and mineralogical composition of these cements, as well as the water content required for each castable in order to attain a suitable moulding under vibration (80% of initial vibration flow).

In general, cements A and D can be directly correlated as they are very close regarding their chemical and mineralogical characteristics, whereas cements B and D show different mineralogy and particle size distribution. Cements A–D are dispersant free, according to their data sheets. Conversely, cement E is a blend of calcium aluminates, reactive alumina and admixtures [17,18]. As a consequence, the water content when using cement E was the highest one. The lowest water content was attained for cement B, most likely due to its bimodal particle size distribution (PSD), resulting in a better castable overall PSD.

After defining the water content for vibratable castables, they were cast into 40 mm × 40 mm cylindrical moulds and the mechanical strength was evaluated after curing at 50 °C (in humid environment) at different time lengths (1, 3, 5 and 7 days). Mechanical strength tests were also carried out after firing at intermediate temperatures (1 day curing at 50 °C, 1 day drying at 110 °C and a dwell time of 5 h at 350, 600, 800 and 1000 °C after a heating rate of 1 °C/min). The mechanical evaluation was conducted according to the ASTM C496-90 standard (Splitting Tensile Strength of Cylindrical Concrete Specimens) in MTS testing equipment (MTS Systems, Model 810, USA).

Table 1
Chemical analysis, physical properties and mineralogical composition of the evaluated cements, and the water content of the castable for each cement source. These data were supplied by the producers.

| Cement source | A | B | C | D | E |
|---|---|---|---|---|---|
| *Chemical analysis (wt.%)* | | | | | |
| $Al_2O_3$ | ≥68.5 | 72 | 72 | 71 | ≥78.1 |
| CaO | ≤31.0 | 27 | 27 | 28 | ≤21.4 |
| $Na_2O$ | <0.5[a] | 0.2 | 0.2 | 0.2 | <0.7[a] |
| $SiO_2$ | <0.8 | 0.2 | 0.2 | 0.2 | ≤0.4 |
| $Fe_2O_3$ | ≤0.3 | 0.1 | 0.1 | 0.1 | ≤0.3 |
| MgO | <0.5 | 0.2 | 0.2 | 0.2 | <0.5 |
| *Physical properties* | | | | | |
| SSA ($m^2/g$) | 1.2 | 1.9 | 2.9 | 1.4 | 5.8 |
| $D_{50}$ (μm) | 13 | 6 | 7 | 13 | 10 |
| *Mineralogical composition* | | | | | |
| CA | Main | Main | Main | Main | Main |
| $CA_2$ | Minor | Minor | – | Minor | Minor |
| $C_{12}A_7$ | – | – | – | – | – |
| α-$Al_2O_3$ | – | Minor | – | – | Minor |
| *Water content in the castable (wt.%)* | | | | | |
| | 4.1 | 3.8 | 4.1 | 4.4 | 4.7 |

[a] For cements A and E, the amounts 0.5 and 0.7 wt.% are related to the sum of $Na_2O + K_2O$.

Thermogravimetric analyses were conducted up to 600 °C at a heating rate of 10 °C/min, on castables cured for 1 day at 50 °C in order to evaluate the drying profile. The thermogravimetric device was developed in the authors' research group and the mass loss during drying ($W$) and the drying rate ($dW/dt$) were calculated as parameters to understand the different drying behavior for the distinct cement sources [19,20].

Following that, samples were moulded (25 mm × 25 mm × 150 mm) to evaluate the cold (CMOR) and hot (HMOR) modulus of rupture (3-point bending tests) after firing at 1150, 1300 and 1500 °C for 5 h (heating rate = 1 °C/min). The CMOR was measured in the MTS apparatus mentioned above according to the ASTM C133-94 standard, whereas the HMOR tests were performed at three different temperatures (1150, 1300 and 1450 °C) (Neztsch, Germany) in HBTS 422 equipment

SEM analyses were conducted using a JEOL JSM-5900 LV microscope. The apparent porosity of the fired samples (for samples fired at intermediate or high temperatures) was also evaluated using the Archimedes technique in kerosene.

In order to assess spinel and $CA_6$ formation expansion, an assisted sintering technique was carried out in refractoriness-under-load equipment (Model RUL 421E, Netzsch, Germany). Cylindrical samples were prepared according to the 51053 DIN standard, cured at 50 °C and dried at 110 °C for 1 day, followed by pre-firing at 600 °C for 5 h before testing. For this test, samples were heated up to 1500 °C under a heating rate of

3 °C/min and kept at this temperature for 5 h. The compression load applied was 0.02 MPa. Creep tests were also performed in samples previously calcined at 600 °C and fired at 1550 °C for 24 h. The creep measurements were carried out at 1450 °C for 24 h under a constant compression load of 0.2 MPa.

## 3. Results and discussion

Fig. 1 shows the mechanical strength behavior for the castables containing different cement sources after curing at 50 °C. Among them, cement C developed the highest mechanical strength level, which is in accordance with its fast setting behavior detected in previous work [21]. The best mechanical strength on curing can be a consequence of a proper $CA/CA_2$ ratio, which could also lead to a greater hygroscopic behavior when compared to cements C and D [21]. The cement mineralogy also plays an essential role in the castable's setting and the higher the amount of $C_{12}A_7$ and CA, the faster the setting. As CA is the only phase detected by X-ray analysis in cement C, it developed the highest strength after a shorter hydration time [22].

Cements A and B also presented suitable curing mechanical strength, whereas cement D did not perform as well, displaying the lowest mechanical strength among all 70 wt.% $Al_2O_3$-containing cements. Although cement A has no further alumina addition, it presents a specific surface area lower than cement B and requires a higher content of water for suitable shaping (4.1 wt.% for A and 3.9 wt.% for B), it showed similar curing behavior to cement B. Comparing cements B and D, B is known as a second generation of cement D (it is finer, has a different mineralogy – higher amount of CA – and results in lower castable water content) and thus led to better mechanical resistance than D.

Concerning cement E, it showed the lowest mechanical strength during curing, which was expected due to its lower lime content and higher water demand (4.7 wt.%). Nevertheless, it was kept under evaluation for the following results due to the benefits that it could provide at high temperatures as it contains a higher amount of alumina.

The castables' drying step was also affected by the different cement sources. The drying rate profile as a function of the sample's temperature (Fig. 2) points out how deeply the castable drying is affected by the cement source, showing differences in the three drying stages [19,20]: evaporation (in the range of room temperature up to 100 °C), ebullition (110–200 °C) and decomposition of cement and magnesia hydrates (above 200 °C). According to Kopanda and MacZura [23], $AH_3$ decomposes in the temperature range of 210–240 °C and $C_3AH_6$ between 240 and 370 °C. Regarding the release of free water, cements B and E were the ones that released water vapour at lower temperatures. This could indicate the likelihood of lower spalling, if the mechanical strength of C was not the lowest among the 70 wt.% alumina cement. Cement E required the highest amount of water for suitable shaping (4.7 wt.%) and led to the highest green apparent porosity level, as will be discussed below.

For cements A and C, the water release took place at higher temperatures and a third peak (close to 500 °C) was detected and is associated with the brucite ($Mg(OH)_2$) decomposition. Previous work by the authors [24] compared castables containing cement A with or without magnesia and this peak was detected only for the magnesia-containing composition. Parr et al. [1] stated that, although the stability domain of brucite at atmospheric pressure is limited to 400 °C, its temperature decomposition can be shifted to 500 °C or above at a higher pressure, which is most likely the condition of well packed refractory castables. One of the main reasons for the formation of brucite in both cements is their lower permeability indicated by the end of the ebullition peak at about 250 °C,

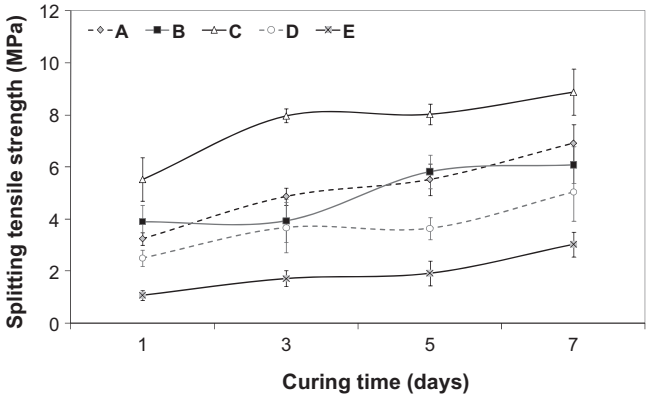


Fig. 1. Splitting strength with the curing time at 50 °C for alumina–magnesia castables containing different cement sources.

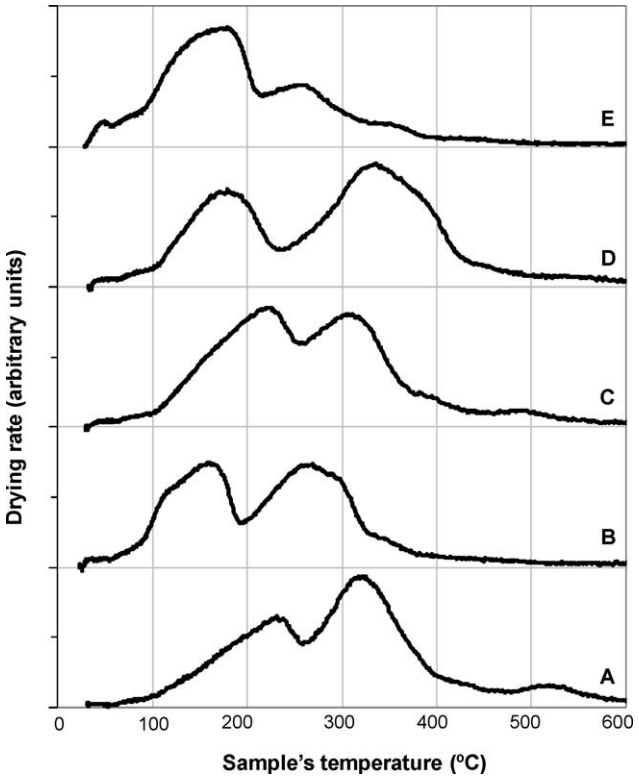


Fig. 2. Drying rate as a function of sample's temperature for alumina–magnesia castables containing different cement sources.

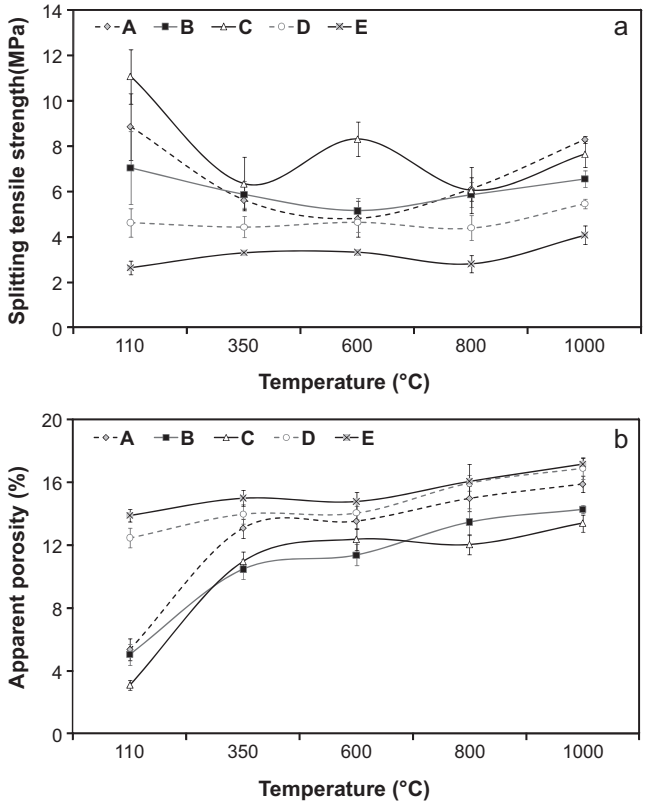


Fig. 3. (a) Splitting strength and (b) apparent porosity after drying at 110 °C and firing for 5 h at intermediate temperatures (from 350 to 1000 °C) for alumina–magnesia castables containing different cement sources.

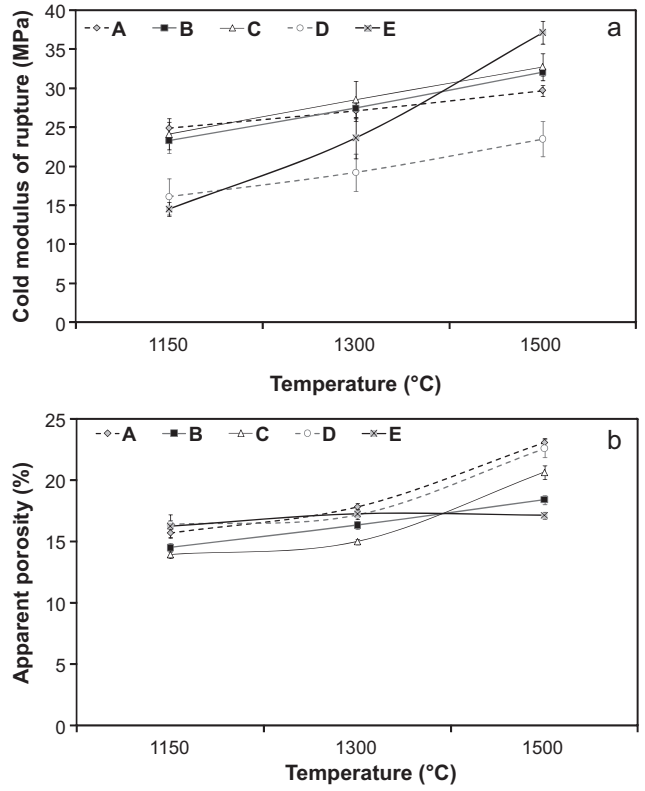


Fig. 4. (a) Modulus of rupture (CMOR) and (b) apparent porosity after firing for 5 h at high temperatures (1150, 1300 and 1500 °C) for alumina–magnesia castables containing different cement sources.

resulting in higher vapour pressure inside the castable and increasing the likelihood for brucite formation.

At intermediate temperatures (110–1000 °C), a mechanical strength loss is commonly detected due to the hydrate decomposition [1,3]. This aspect is pointed out in Fig. 3a for compositions containing cements A and B, which showed a drop in the splitting tensile strength up to 600 °C, followed by its increase up to 1000 °C. As detected during curing, cement C also presented higher mechanical strength in this temperature range. Unlike cements A, B and C, cement D showed a lower splitting tensile strength level for all fired temperatures. Fig. 3b points out the high apparent porosity level of the composition containing cement D, which is mainly related to the high water content required for this castable. Similar behavior was detected for cement E-containing castable: low mechanical strength and high initial apparent porosity. Nevertheless, from 800 to 1000 °C, an increase in the mechanical strength took place, most likely due to the sintering start-up process, as this source of cement contains additional reactive alumina in its composition.

The sintering effect of cement E is highlighted in Fig. 4, which shows the mechanical strength and apparent porosity for the samples fired at 1150, 1300 and 1500 °C for 5 h. Although it displayed the lowest mechanical strength at intermediate

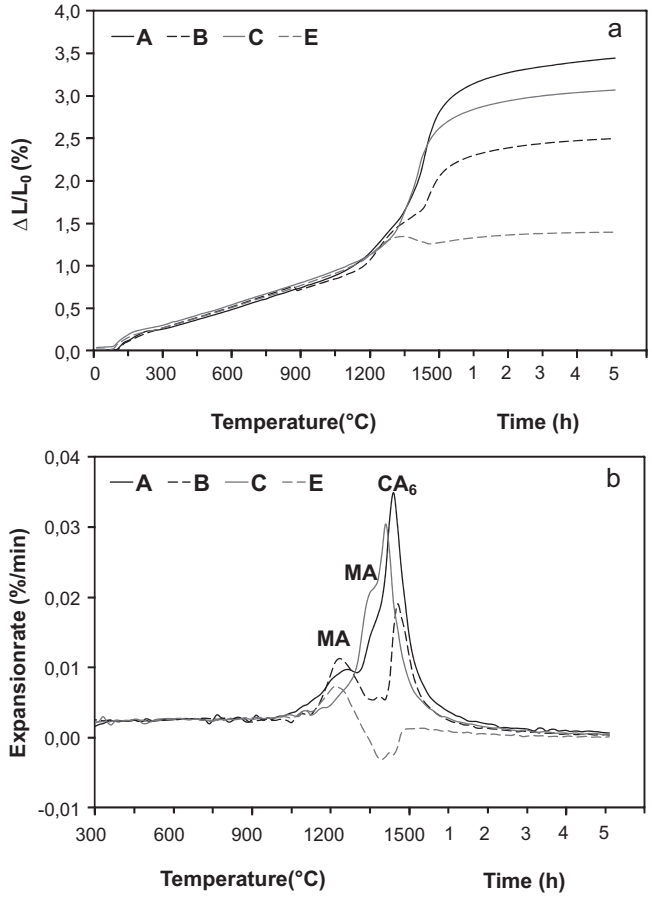


Fig. 5. (a) Linear expansion and (b) expansion rate during the assisted sintering test (up to 1500 °C, dwell time of 5 h) for alumina–magnesia castables containing different cement sources. MA: $MgAl_2O_4$.

temperatures and after firing at 1150 °C, this property value increased and, at 1500 °C, cement E showed the highest mechanical strength level and the lowest apparent porosity among all cements. Besides sintering, this result is also a consequence of lower calcium hexaluminate ($CA_6$) generation, as this cement comprises less calcia than the others. According to previous work by the authors [12], an excessive $CA_6$ formation could result in cracks and deteriorate the castable's properties.

For the 70 wt.% CaO-containing cements (A–D), cements A–C behaved similarly in terms of mechanical strength (a slight advantage for cements B and C), but cement C showed lower apparent porosity level, indicating higher sinterability. Conversely, cement D showed similar apparent porosity than cement A, but lower mechanical strength. This aspect indicates a lack of bonding effects of cement D and, as it did not perform as well as the others for all processing steps (curing, drying and sintering), it was not included for further evaluations (assisted sintering—expansion behavior, hot modulus of rupture and creep resistance).

The assisted sintering technique results (Fig. 5) indicated different expansion behavior when changing the cement source. Among all of them, cement E resulted in the lowest expansion level, pointing out its sinterability. Furthermore, as it contains less CaO than the other sources, the calcium hexaluminate content of this composition is lower. Taking into account the spinel ($MgAl_2O_4$) and $CA_6$ expansion rate peaks [12], not only the calcium hexaluminate peak (almost undetectable for this cement) was reduced, but also the spinel one, as shown in Fig. 5b. Therefore, the fine alumina added to this cement played an important role, accommodating both spinel and $CA_6$ expansion.

Although the expected $CA_6$ content for cement E is lower, this phase was detected by SEM analyses after sintering at 1500 °C for 5 h, as for the other cements (Fig. 6). The calcium hexaluminate morphology was similar for all compositions (mainly needle-like grains), but its location was different. For the 70-wt.% $Al_2O_3$ cement sources, $CA_6$ needles were detected at the edge of tabular alumina grains (TA) and also in the castables' matrix. Conversely for the 80-wt.% $Al_2O_3$ cement (E), $CA_6$ was mainly detected inside the tabular alumina grains.

Comparing the cement sources containing 70 wt.% of CaO (A–C), cements A and C showed the highest expansion levels (slightly higher for cement A), but due to different reasons. Whereas cement A showed a higher $CA_6$ expansion rate peak, cement C had the highest spinel one. This result highlights the cement source effect on the different expansion reactions and, thus, the importance of a proper cement selection as it would affect not only the initial processing steps, but also the reactions taking place at high temperatures. Concerning cement B, the expansion level was intermediate and, although its sintering performance was not as effective as the one detected for cement E, it showed similar behavior to the 80 wt.% CaO-containing cement (E): low spinel expansion rate peak, followed by a well due to sintering and $CA_6$ peak. The clear identification of the spinel and $CA_6$ expansion peaks at different temperature ranges for cement C suggests that either the spinel formation was speeded up due to the alumina added to this cement or the sintering effect prevailed over the spinel expansion.

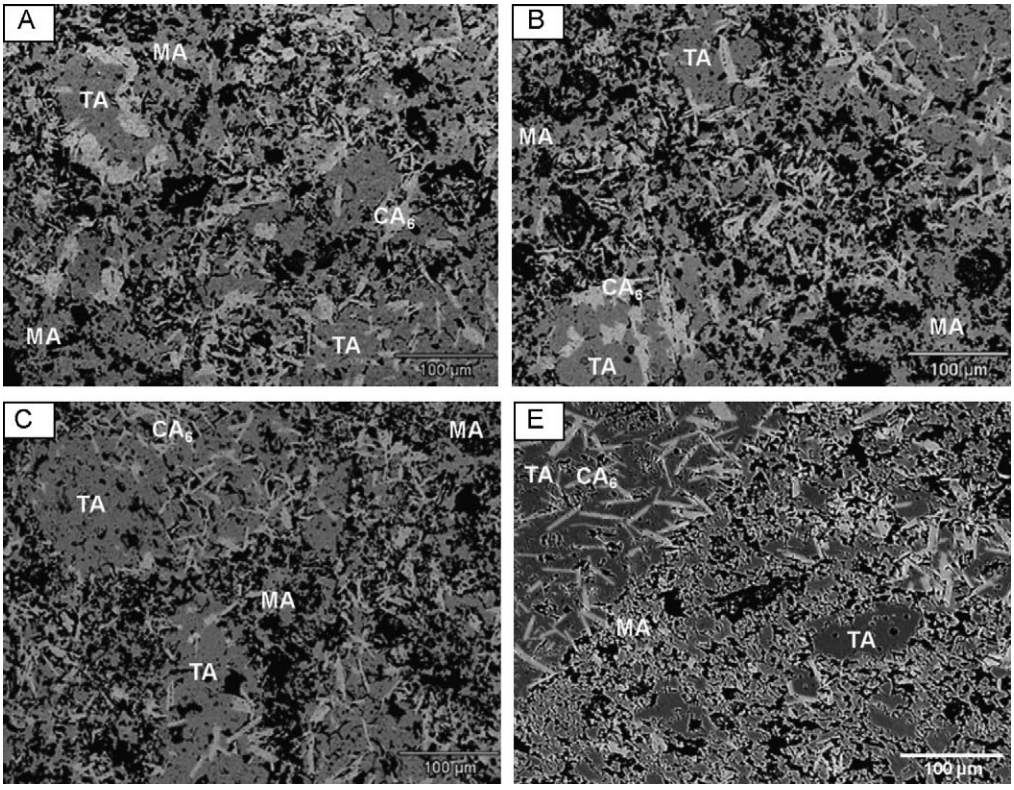


Fig. 6. SEM images for alumina–magnesia castables containing different cement sources, after firing at 1500 °C for 5 h. MA: $MgAl_2O_4$, TA: tabular alumina and $CA_6$ is the brighter phase, with needle-like morphology.

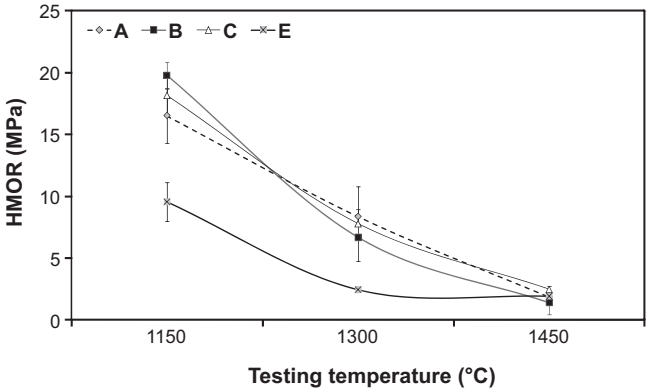


Fig. 7. Hot modulus of rupture (HMOR) at different testing temperatures (1150, 1300 and 1450 °C) for alumina–magnesia castables containing different cement sources.

Considering that one of the main advantages of reducing the CaO content in the castable compositions is associated with the hot properties (low melting point phase generation could be avoided [3]), hot modulus of rupture and creep resistance measurements were carried out. Fig. 7 shows the HMOR results for samples previously fired at 1150, 1300 and 1500 °C for 5 h and evaluated at 1150, 1300 and 1450 °C (this former temperature was selected instead of 1500 °C, due to the maximum working temperature of the HMOR equipment). At lower temperatures (1150 and 1300 °C), the 70 wt.% CaO-containing cements showed higher hot mechanical resistance, as presented for the cold modulus of rupture results (Fig. 4). Moreover, in spite of the lowest CaO amount in cement E, the HMOR level at 1450 °C was similar (and low) for all compositions. This result is a consequence of the castable microsilica content, which was the same for all compositions (1 wt.%).

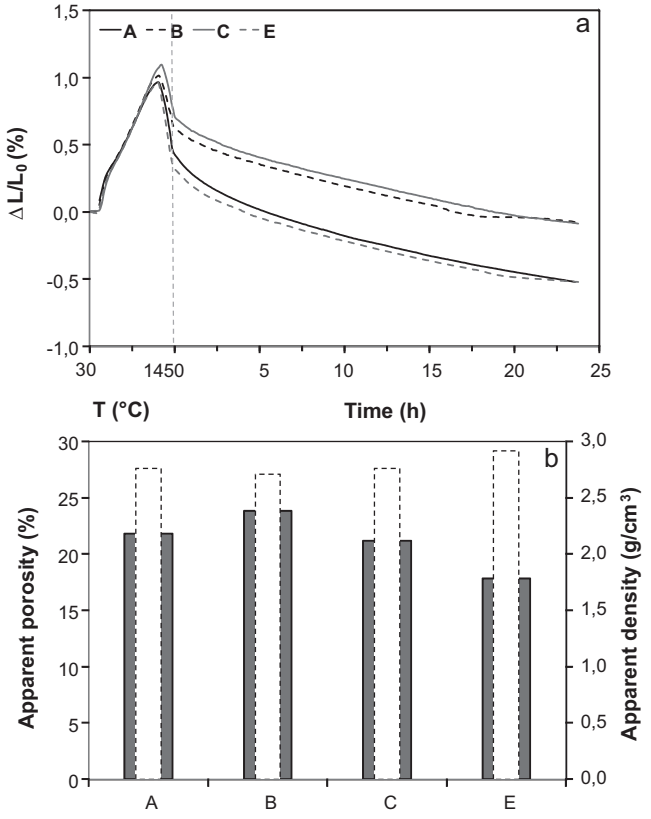


Fig. 8. (a) Creep deformation at 1450 °C for 24 h under compression load of 0.2 MPa and (b) apparent porosity and density for alumina–magnesia castables containing different cement sources, previously pre-fired at 1550 °C for 24 h.

After evaluating the HMOR, creep tests were carried out at 1450 °C for 24 h (for samples previously fired at 1550 °C for 24 h, in order to inhibit sintering during the experiment). The results attained are shown in Fig. 8a. Taking into account that cement E experienced the lowest apparent porosity and the highest apparent density (Fig. 8b), and comprises less lime than the others (20 wt.% instead of 30 wt.% of CaO), better creep resistance would be expected (lower deformation). Nevertheless, this result was not attained and there was a clear trend: the cements of the same producer (A–E and B and C) resulted in similar creep behavior, regardless of the apparent porosity and density levels. The best creep performance was attained for cements B and C. According to Stinessen et al. [14], the purity of raw materials and the $C_{12}A_7$ content (added in minor amounts (<1 wt.%) to speed up setting) are essential for designing properties, mainly the hot ones and, thus, can influence the creep results.

## 4. Conclusions

Considering that the cement sources displayed different behaviors during the overall processing steps, attention should be drawn to the cement source selection, as this raw material affects the overall performance of alumina–magnesia refractory castables. Concerning the cement containing a lower lime content (20 wt.% of CaO, cement E), advantages in terms of expansion and microstructural design were detected, but the expected hot properties benefits were not attained, indicating that cement setting phases ($C_{12}A_7$) and other castables raw materials, such as microsilica should be considered when designing the composition of this sort of castables. Comparing the cements containing 30 wt.% of lime (A–D), two of them (B and C) showed not only good mechanical strength, but also an outstanding creep resistance. Nevertheless, as the expansion levels were different for each cement source, the proper selection of the most suitable cement should be carried out. Therefore, the refractory castable should be designed in terms of the cement source according to the application requirements, considering which of them are the priorities (fast demoulding, fast drying, low expansion level, high mechanical strength at intermediate temperatures, creep resistance and so on). As the priorities are established, the results presented in this paper could be used as a cement source property road-map, in order to fulfill the requirements during the castable's use.

## Acknowledgments

The authors are grateful to the Federation for International Refractory Research and Education (FIRE), Magnesita Refratários S.A. (Brazil), Corus—Ceramics Research Centre

(The Netherlands) and the Brazilian Research Funding Agency FAPESP for supporting this work.

## References

[1] C. Parr, L. Bin, B. Valdelievre, C. Wöhrmeyer, B. Touzo, The advantages of calcium aluminate cement containing castable for steel ladle application, in: Proceedings of XXXII ALAFAR Congress, 2004, p. 14.
[2] N. Zhou, S. Hu, S. Zhang, Advances in modern refractory castables, China's Refractories 13 (2) (2004) 3–12.
[3] W.E. Lee, W. Vieira, S. Zhang, A. Ghanbari, H. Sarpoolaky, C. Parr, Castable refractory concretes, International Materials Review 46 (3) (2001) 145–167.
[4] M.A.L. Braulio, L.R.M. Bittencourt, V.C. Pandolfelli, Selection of binders for *in situ* spinel refractory castables, Journal of the European Ceramic Society 29 (2009) 2727–2735.
[5] R. Salomão, V.C. Pandolfelli, The role of hydraulic binders on magnesia containing refractory castables: calcium aluminate cement and hydratable alumina, Ceramics International 35 (2009) 3117–3124.
[6] Y.C. Ko, J.T. Lay, Thermal expansion characteristics of alumina–magnesia and alumina–spinel castables in the temperature range 800–1650 °C, Journal of the American Ceramic Society 83 (11) (2000) 2872–2874.
[7] M.A.L. Braulio, J.F.R. Castro, C. Pagliosa, L.R.M. Bittencourt, V.C. Pandolfelli, From macro to nanomagnesia: designing the *in situ* spinel expansion, Journal of the American Ceramic Society 91 (9) (2008) 3090–3093.
[8] M.A.L. Braulio, M.F.L. Piva, G.F.L. Silva, V.C. Pandolfelli, Spinel expansion design by colloidal alumina suspension addition, Journal of the American Ceramic Society 92 (2) (2009) 559–562.
[9] M.A.L. Braulio, L.R.M. Bittencourt, V.C. Pandolfelli, Engineered expansion routes for alumina–magnesia castables, Ceramic Forum International 85 (10) (2008) E21–E26.
[10] J.M. Auvray, C. Gault, M. Huger, Evolution of elastic properties and microstructural changes versus temperature in bonding phases of alumina and alumina–magnesia refractory castables, Journal of the European Ceramic Society 27 (2007) 3489–3496.
[11] K. Ide, T. Suzuki, K. Asano, T. Nishi, T. Isobe, H. Ichikawa, Expansion behavior of alumina–magnesia castables, Journal of the Technical Association of Refractories—Japan 25 (3) (2005) 202–208.
[12] M.A.L. Braulio, D.H. Milanez, E.Y. Sako, L.R.M. Bittencourt, V.C. Pandolfelli, Expansion behavior of cement bonded alumina–magnesia refractory castables, American Ceramic Society Bulletin 86 (12) (2007) 9201–9206.
[13] M.A.L. Braulio, L.R.M. Bittencourt, J. Poirier, V.C. Pandolfelli, Microsilica effects on cement bonded alumina–magnesia refractory castables, Journal of the Technical Association of Refractories—Japan 28 (3) (2008) 180–184.
[14] I. Stinessen, A. Buhr, R. Kockegey-Lorenz, R. Racher, High purity calcium aluminate cements, production and properties. Available from: <http://www.almatis.com/refractory/technical-papers.aspx> (accessed 02.2010).
[15] L. Krietz, Refractory castables, in: C.A. Schacht (Ed.), Refractories Handbook, Marcel Dekker, Inc., USA, 2004, pp. 259–284.
[16] J.E. Funk, D.R. Dinger, Particle packing, part III: discrete versus continuous particles sizes, Interceram 41 (5) (1992) 332–333.
[17] Secar® 71 and Secar® 80 Product Datasheets. Available from: <http://www.kerneosinc.com/index2.php> (accessed 02.2010).
[18] Almatis Calcium Aluminate Cement Datasheets. Available from: <http://www.almatis.com/refractory/applications/cements-and-binders.aspx> (accessed 02.2010).
[19] M.D.M. Innocentini, F.A. Cardoso, A.E.M. Paiva, V.C. Pandolfelli, Dewatering refractory castables, American Ceramic Society Bulletin 83 (7) (2004) 9101–9108.
[20] M.D.M. Innocentini, F.A. Cardoso, M.M. Akyioshi, V.C. Pandolfelli, Drying stages during the heating of high-alumina, ultra-low cement refractory castables, Journal of the American Ceramic Society 86 (7) (2003) 1146–1148.
[21] A. Buhr, D. Schmidtmeier, G. Wams, D. Zacherl, J. Dutton, New results for CA-470 TI temperature-independent cement—robustness against low temperatures and impurities, in: Proceedings of UNITECR'09, 2009, 6 p..
[22] A. Buhr, D. Gierisch, H. Groβ, F. Kraaijenbos, G. Wams, J. Dutton, A new temperature independent cement for low and ultra low cement castables, in: Proceedings of UNITECR'07, 2007, 5 p..
[23] J.E. Kopanda, G. Maczura, Production processes, properties, and applications for calcium aluminate cements, in: L.D. Hart (Ed.), Alumina Chemicals, Science and Technology Handbook, 1990, 171–184.
[24] M.A.L. Braulio, D.H. Milanez, E.Y. Sako, L.R.M. Bittencourt, V.C. Pandolfelli, The effect of calcium aluminate cement on the in-situ spinel expansion, in: Proceedings of UNITECR'07, 2007, 4 p..